2,6-dimethyl-4-nitrophenolate in intimate contact with the 2,3-hydroxyl groups. The ^{13}C T_1 data shows that the methylated sodium nitrophenolate is more tightly coupled to the cavity than parent sodium nitrophenolate, $\xi = 0.41$ vs. $\xi = 0.13$. This coupling is likely due to an interaction between the substrate's methyl groups and the cavity's 2,3-hydroxyl groups. This interaction is further evidenced by a decrease in the spin rate of the substrate's methyl groups on cycloamylose complexation. This evidence implies that the acyl group of 3-nitrophenyl acetate would be very close to the active 2-hydroxyl group if the substrate bound in the cavity nitro group first at the 2,3-hydroxyl side. Furthermore, if methyl groups are so effective in increasing cycloamylose substrate coupling the somewhat larger acyl groups should be even more effective in assisting cycloamylose substrate coupling.

Consequently, the observation that 3-nitrophenyl acetate is deacylated by cyclohexaamylose faster than the 4-nitrophenyl acetate can be attributed to both the steric relationship of the reactive groups and at least in part to the reduced motion of the substrate. The origins of the small catalytic effect observed in the deacylation of the 4-nitrophenyl acetate by cyclohexaamylose must be attributed to some mechanism other than that suggested in the literature.[2,10] The 4-nitrophenyl acetate must either penetrate the cavity more deeply than the corresponding sodium 4-nitrophenolate on cyclohexaamylose complexation, or the aromatic ring of 4-nitrophenyl acetate must improve on the leaving ability of the 4-nitrophenolate. This stabilization of the leaving group has some basis in the observation that the pK_a of 4-nitrophenol is 1 pK_a unit lower when complexed by cyclohexaamylose.[27]

Conclusion

The results suggest that the cyclohexaamylose deacylations of 4-nitrophenyl and 3-nitrophenyl acetate proceed by different mechanisms. The present evidence as well as recent X-ray studies shows that, unless the 4-nitrophenyl acetate penetrates the cyclohexaamylose cavity substantially further than the corresponding nitrophenol or nitrophenolate, its acyl group is simply too far from the cyclohexaamylose's catalytic 2-hydroxyls to react. An alternative explanation of the observed catalytic effect suggested by pK_a studies is that the complexation of the nitrophenol segment of 4-nitrophenyl acetate increases the stability of the leaving group.[27]

Acknowledgment. We wish to acknowledge the Alfred P. Sloan Foundation and the Cottrell Research Corporation for their generous support of this research. We also wish to acknowledge Dr. Cherie Fisk of the National Institutes of Health for her help with computer analysis of the ^{13}C relaxation data.

References and Notes

(1) R. J. Bergeron, *J. Chem. Educ.*, **54**, 204 (1977).
(2) D. W. Griffiths and M. J. Bender, *Adv. Catal.*, **23**, (1973).
(3) N. Nakamura and K. Horikoshi, *Agric. Biol. Chem.*, **40**, 935 (1976).
(4) K. Vekama, M. Otagiu, Y. Kamie, S. Tanaka, and K. Ikeda, *Chem. Pharm. Bull.*, **23**, 1421 (1975).
(5) R. Gelb, L. M. Schwartz, C. T. Murray, and D. A. Laufer, *J. Am. Chem. Soc.*, **100**, 3553 (1978).
(6) Y. Kitawa and M. L. Bender, *Bioorg. Chem.*, **4**, 237 (1975).
(7) B. Siegel, A. Penter, and R. Breslow, *J. Am. Chem. Soc.*, **99**, 2309 (1977).
(8) J. Emert and R. Breslow, *J. Am. Chem. Soc.*, **97**, 670 (1975).
(9) Y. Kitawa and M. Bender, *Bioorg. Chem.*, **4**, 237 (1975).
(10) R. L. Van Etten, J. F. Sebastian, G. A. Clowes, and M. L. Bender, *J. Am. Chem. Soc.*, **89**, 3242 (1967).
(11) P. K. Glasoe and F. A. Long, *J. Phys. Chem.*, **64**, 188 (1960).
(12) R. J. Bergeron, M. A. Channing, G. J. Gibeily, and D. M. Pillor, *J. Am. Chem. Soc.*, **99**, 5146 (1977).
(13) D. Canet, G. C. Levy, and I. R. Peat, *J. Magn. Reson.*, **18**, 199 (1975).
(14) G. C. Levy, and I. R. Peat, *J. Magn. Reson.*, **18**, 500 (1975).
(15) J. D. Behr and J. M. Lehn, *J. Am. Chem. Soc.*, **98**, 1743 (1976).
(16) J. E. Anderson and D. A. Fryer, *J. Chem. Phys.*, **50**, 3784 (1969).
(17) G. C. Levy, J. D. Cargioli, and F. A. L. Anet, *J. Am. Chem. Soc.*, **95**, 1527 (1973).
(18) T. L. James, "Nuclear Magnetic Resonance in Biochemistry", Academic Press, New York, 1975.
(19) J. H. Noggle and R. E. Schirmer, "The Nuclear Overhauser Effect", Academic Press, New York, 1971.
(20) C. H. Brevard, J. P. Kintzinger, and J. H. Lehn, *Tetrahedron*, **28**, 2447 (1972).
(21) P. Colson, H. J. Jennings, and I. C. P. Smith, *J. Am. Chem. Soc.*, **96**, 8081 (1974).
(22) R. Bergeron and M. Channing, *Bioorg. Chem.*, **5**, 437 (1976).
(23) R. Bergeron and R. Rowan, *Bioorg. Chem.*, **5**, 425 (1976).
(24) D. Laufer, private communication.
(25) R. Bergeron, M. Channing, W. P. Roberts, and K. McGovern, *Bioorg. Chem.*, in press.
(26) K. Harata, *Bull. Chem. Soc. Jpn.*, **50**, 1416 (1977).
(27) K. A. Connors and J. M. Lipari, *J. Pharm. Sci.*, **65**, 379 (1976).

Electron Spin Resonance Studies on Radiolysis of Crystalline Methanol at 4.2 K

Kazumi Toriyama and Machio Iwasaki*

Contribution from Government Industrial Research Institute, Nagoya Hirate, Kita, Nagoya, Japan. *Received October 3, 1978*

Abstract: Radiolysis of crystalline methanol and the structure of radicals produced have been studied at 4.2 K using electron spin resonance spectroscopy. It has been observed for the first time that $CH_3\dot{O}$ and $\dot{C}H_3$ are formed as major products together with conventional $\dot{C}H_2OH$ in pure CH_3OH irradiated at 4.2 K. The direct evidence was obtained that both $CH_3\dot{O}$ and $\dot{C}H_3$ convert into $\dot{C}H_2OH$ below 77 K. Intramolecular hydrogen atom transfer is suggested for the conversion from $CH_3\dot{O}$ into $\dot{C}H_2OH$. Besides these isolated radicals, considerable amounts of radical pairs between $\dot{C}H_3$ and $\dot{C}H_2OH$ were formed. $\dot{C}H_3$ in this pair also converts into $\dot{C}H_2OH$ forming radical pairs between $\dot{C}H_2OH$ below 77 K. The change in the radical pair separation indicates that CH_3 abstracts a hydrogen atom from the neighboring CH_3 group forming $\dot{C}H_2OH$. It is suggested that the radical pairs are formed from recombination of an electron and a cationic species. The electronic and geometrical structure of $CH_3\dot{O}$ has also been discussed. The radical is the oxygen-centered π radical and the CH_3 group undergoes tunneling rotation at 4.2 K. From the A- and E-line splittings, B_0 and B_2 in the $\cos^2\theta$ rule for the β proton coupling in the oxygen-centered π radicals have been estimated to be 5 and 94 G, respectively.

In recent years, we have been studying the solid-state radiolysis of organic compounds at cryogenic temperatures (4.2 K) with electron spin resonance (ESR) spectroscopy.[1-5] It becomes gradually clear that the solid-state radiolysis at temperatures lower than 77 K involves two important phases: the one is that migration of hydrogen atoms produced by ra-

0002-7863/79/1501-2516$01.00/0

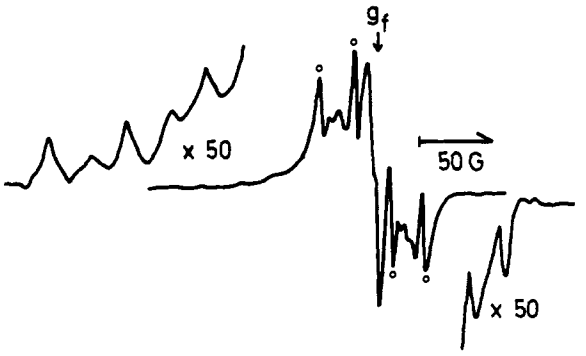

Figure 1. ESR spectra of polycrystalline CH_3OH X-irradiated and measured at 4.2 K. The overlay spectrum is measured with 50 times higher gain. The open circles indicate the lines due to $\dot{C}H_3$. The arrow indicates the position of a DPPH marker. The microwave power = 6 μW, field modulation width = 1.5 G.

diolysis is greatly suppressed at 4.2 K[1,3] and the other is that the hydrogen atom transfer reactions proceed even at 4.2 K by the tunnel effect.[4,5] These factors lead to a different radiation effect on saturated hydrocarbons at quite low temperatures.[1-3] In the present study, we have studied the low-temperature radiolysis of methanol, which is one of the most important and fundamental organic substances in radiation chemistry.

The radiolysis of methanol has been extensively studied in the liquid and solid phases.[6,7] However, most solid-phase studies have been made using glassy samples containing a small amount of water. In this work, we have mainly studied polycrystalline methanol irradiated at 4.2 K. It has been found that primary radicals such as $CH_3\dot{O}$ and $\dot{C}H_3$ can be trapped at 4.2 K as major products together with familiar $\dot{C}H_2OH$. Besides these isolated radicals, it has been found that considerable amounts of radical pairs between $\dot{C}H_3$ and $\dot{C}H_2OH$ are formed. The preliminary results, especially on the first observation of $CH_3\dot{O}$, have been reported in our previous communication.[8] In this paper, the details of our experiments and analysis will be given together with the radiation chemical aspects of the formation of $\dot{C}H_3$ as one of the important primary species and of the formation of isolated and paired radicals in crystalline methanol.

Experimental Section

Samples of CH_3OH (spectrograde) were obtained from Wako Pure Chemical Ltd., and those of CH_3OD and CD_3OD from Merck Sharp and Dohme Ltd. The samples were purified in a vacuum line by molecular sieves 3A to eliminate water and then distilled into an ESR sample tube. The samples were carefully crystallized in an ESR tube by slow cooling. Bad crystals containing glassy phases colored after irradiation indicating formation of trapped electron in the glassy phases. The results presented in this paper were obtained from good crystals which did not color after irradiation. The samples were kept in direct contact with liquid helium in a Dewar and were irradiated by X-rays (45 kV, 40 mA) for 15 min to a dose of about 1.7×10^5 rad. The insersion-type liquid helium Dewar was engaged with an ESR cavity after irradiation and the spectra were measured by a Varian E-12 spectrometer with 100-kHz field modulation. The details of our experimental setup for the low-temperature irradiation and ESR measurements have already been reported in our previous paper [2] ESR spectra were digitized and integrated by a Nicolet 1070 signal averager.

Results

ESR Spectra of Isolated Radicals. Figures 1, 2, and 3 show the ESR spectra of polycrystalline CH_3OH, CH_3OD, and CD_3OD X-irradiated and measured at 4.2 K. The central part of the spectra at $g \approx 2$ is a superposition of the signals arising from methyl and hydroxymethyl radicals, although overlapping of the spectra arising from hydroxymethyl radicals is not

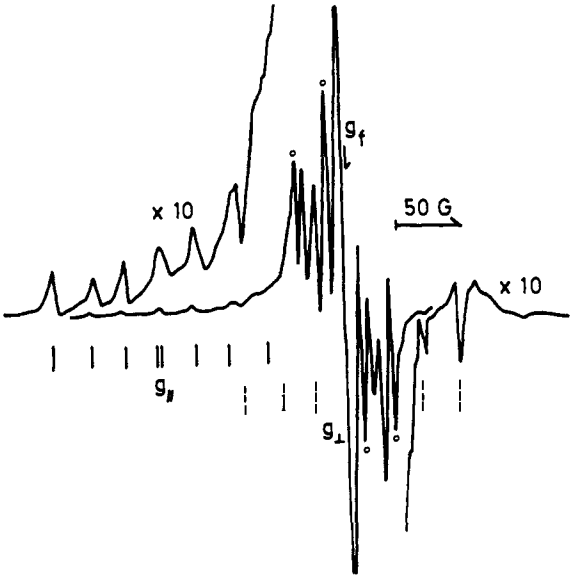

Figure 2. ESR spectra of polycrystalline CH_3OD X-irradiated and measured at 4.2 K. The open circles indicate the lines due to $\dot{C}H_3$. The overlay spectrum is measured with ten times higher gain. The microwave power = 6 μW, field modulation width = 1.5 G.

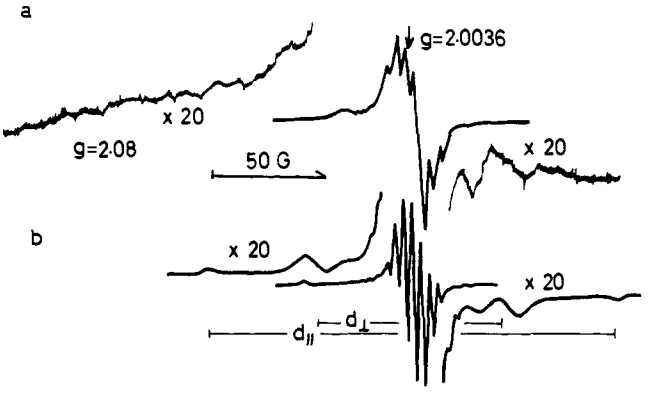

Figure 3. ESR spectra of polycrystalline CD_3OD X-irradiated at 4.2 K: (a) measured at 4.2 K; (b) measured at 77 K. The overlay spectra were measured with 20 times higher gain. The microwave power = 2 μW, field modulation width = 1.5 G.

clear in CD_3OD. It seems that the abundance ratio of methyl to hydroxymethyl radicals is higher in CD_3OD. One of the causes of this difference is in the greater stability of CD_3 radicals, which will be described later. In the case of CH_3OH, the weak signal arising from $\dot{C}HO$ is also seen on the tail of the $\dot{C}H_3$ spectrum as a minor product. The amount is probably less than 1% of the total radical yield. It is to be noted that the crystalline samples carefully prepared do not give a detectable ESR signal from trapped electrons.

The overlay spectra in Figures 1 and 2 measured with higher gain are due to methoxy radicals. The structure in the low-field side is the hyperfine structure of the g_{max} component of the polycrystalline ESR line shape. The seven-line hyperfine structure with an approximately equal spacing can be interpreted in terms of the couplings with the methyl protons which undergo quantum tunneling rotation.[9,10] Although the detailed discussion will be given in a later section, the hyperfine coupling constant of the rotating methyl protons is determined to be 52 G from the A-line splitting. The g_{max} value is obtained as 2.088 from the center of the hyperfine structure. The two lines in the high-field end of the overlay spectrum have just the same spacing as that of the outermost two lines in the low-field hy-

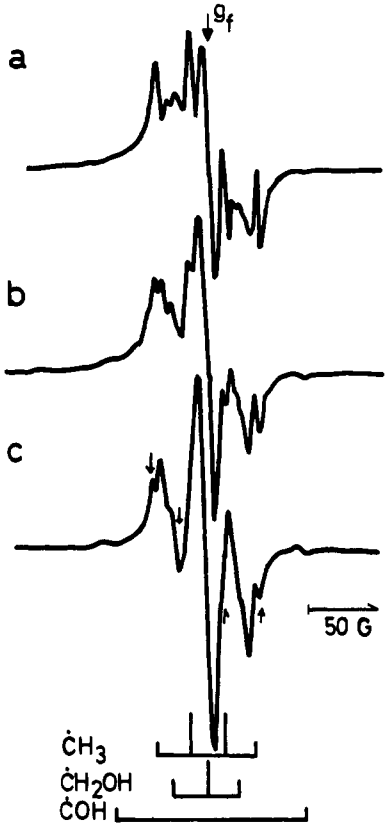

Figure 4. ESR spectral change at 4.2 and 77 K in polycrystalline CH_3OH measured at 4.2 K: (a) 20 min after X-irradiation at 4.2 K; (b) 2 h after X-irradiation at 4.2 K; (c) after annealing at 77 K for 1 min. The arrows in (c) indicate the trace amount of $\dot{C}H_3$ remained after annealing. The arrow marked with g_f indicates a DPPH marker. The spectrometer gain is the same for (a) and (b), and ×0.7 for (c). The microwave power = 6 μW, field modulation = 1.5 G.

perfine lines. This suggests that the two lines are the outermost hyperfine lines in the high-field hyperfine structure on the g_{min} component and this is also consistent with the isotropic nature of a rotating CH_3 β-proton coupling. Although the signal arising from $CH_3\dot{O}$ looks relatively weak, its amount is estimated to be one-third of the total radical yield, because of the wide spreading of the spectra due to g anisotropy. The estimation is based on the spectral simulation of the methoxy radical and the integrated intensity of the entire spectrum. The relative amounts of the three major species, $CH_3\dot{O}$, $\dot{C}H_3$, and $\dot{C}H_2OH$, in CH_3OH are estimated to be 0.3:0.3:0.4. Similar ratios were also obtained from CH_3OD.

As is shown in the overlay spectrum at around $g = 2.08$ in Figure 3, the spectrum supposed to be due to $CD_3\dot{O}$ in CD_3OD is very broad and it is hard to deduce a definite conclusion. The wide spreading (48 G) due to the unresolvable hyperfine coupling expected from the CD_3 deuterons seems to smear out the spectra, making clear identification difficult.

Conversion of $\dot{C}H_3$ and $CH_3\dot{O}$ into $\dot{C}H_2OH$. It has been observed that the signal of $\dot{C}H_3$ gradually decreases with the increase of the signal of $\dot{C}H_2OH$ even at 4.2 K. Figures 4a and 4b show the spectra measured 20 min and 2 h after irradiation at 4.2 K, respectively. The double integration of the spectra shows that there is no appreciable change in the total amount of radicals. In addition, during this change, the signal from $CH_3\dot{O}$ remains unchanged. This clearly indicates that $\dot{C}H_3$ abstracts a hydrogen atom from a neighboring molecule forming $\dot{C}H_2OH$. The half-life of $\dot{C}H_3$ in CH_3OH at 4.2 K is roughly estimated to be 1 h. Although $\dot{C}H_3$ in CH_3OD shows a similar behavior, it seems that the half-life of $\dot{C}H_3$ in CH_3OD is slightly longer than that in CH_3OH.

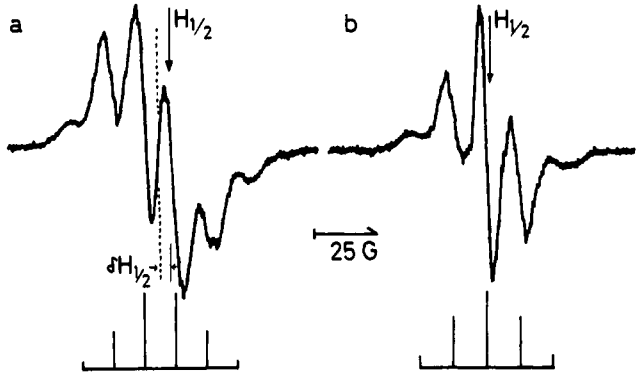

Figure 5. The $\Delta M_s = \pm 2$ spectra of radical pairs formed in CH_3OD X-irradiated at 4.2 K: (a) before annealing; (b) after annealing at 77 K for 5 min. The arrow marked $H_{1/2}$ indicates the position of an exact half-field expected from the allowed transition. $\delta H_{1/2}$ is the shift from $H_{1/2}$. Microwave power = 5 mW, field modulation width = 2.5 G.

Figure 4c shows the spectra of CH_3OH measured at 4.2 K after annealing the crystals at 77 K for 1 min. The signals from $CH_3\dot{O}$ as well as $\dot{C}H_3$ disappear and only the spectrum from $\dot{C}H_2OH$ remains. However, the integrated intensity remains unchanged, suggesting that not only $\dot{C}H_3$ but also $CH_3\dot{O}$ converts into $\dot{C}H_2OH$. A similar change was also observed in CH_3OD.

On the other hand, $\dot{C}D_3$ in CD_3OD is quite stable at 4.2 K and even at 77 K. Figure 3b shows the spectrum of $\dot{C}D_3$ measured at 77 K after irradiation at 4.2 K. The equally spaced seven-line spectrum with the separation of 3.5 G and the binomial intensity ratio is clearly ascribable to $\dot{C}D_3$. The resolution improvement of the spectrum measured at 77 K is mainly due to motional narrowing and the spectrum remeasured at 4.2 K after annealing at 77 K is as broad as that shown in Figure 3a. Although notable conversion from $\dot{C}D_3$ into $\dot{C}D_2OD$ was not observed at 77 K, the broad spectrum supposedly due to $CD_3\dot{O}$ disappeared after annealing at 77 K. It seems that $CD_3\dot{O}$ converts into $\dot{C}D_2OD$ below 77 K. Since the spectrum of $\dot{C}D_2OD$ is considerably broader than that of $\dot{C}D_3$, it was difficult to detect $\dot{C}D_2OD$ formed from $CD_3\dot{O}$. The conversion from $\dot{C}D_3$ into $\dot{C}D_2OD$ was observed after annealing at 138 K for 3 min.

ESR Spectra of Radical Pairs. In order to examine pairwise trapping of radicals in methanol at 4.2 K, we have measured the $\Delta M_s = \pm 2$ transitions which are characteristic of triplet radical pairs.[1,11,12] Figure 5 shows the $\Delta M_s = \pm 2$ spectra obtained from CH_3OD irradiated and measured at 4.2 K. As is shown in Figure 5a, the splitting of the six-line hyperfine structure is about one-half of the hyperfine splitting in the isolated $\dot{C}H_3$ and $\dot{C}H_2OD$ radicals. This is characteristic of spin exchange coupled pairs, in which each electron spends half of the time interacting with nuclei in each paired radicals. The six-line spectrum with the approximately binomial intensity ratio is consistent with the assignment to the radical pair between $\dot{C}H_3$ and $\dot{C}H_2OD$. The spectrum (b) in Figure 5 is measured at 4.2 K after annealing at 77 K for 1 min. It is clearly seen that the six-line spectrum changed into the five-line spectrum with the approximately binomial intensity ratio, which is attributable to the radical pair between $\dot{C}H_2OD$ in which the number of coupling protons is reduced from five to four. A similar change was also observed in CH_3OH, although the resolution of the spectra is considerably poor. This radical pair conversion gives unequivocal confirmation that $\dot{C}H_3$ converts into $\dot{C}H_2OH$. On the other hand, the radical pairs in CD_3OD did not give resolvable hyperfine structures so that clear information was not obtained from the spectral change due to the thermal annealing.

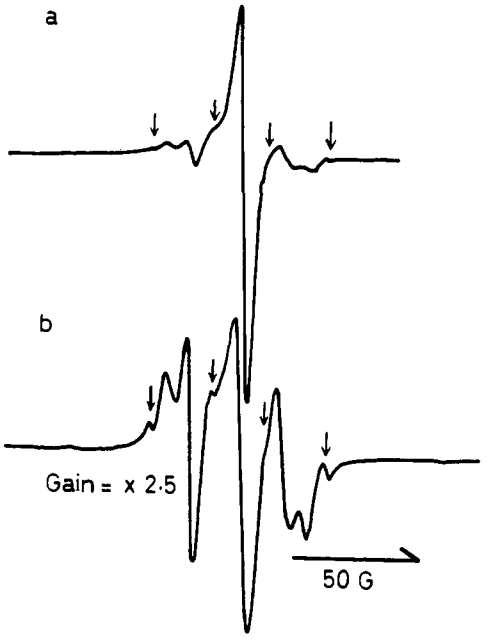

Figure 6. ESR spectra of glassy CH_3OD containing 5 mol % of D_2O X-irradiated and measured at 4.2 K: (a) before photobleaching; (b) after exposing to visible light at 4.2 K for 2.5 min. The arrows indicate the signal arising from $\dot{C}H_3$. The spectrometer gain for (b) is ×2.5 of that for (a). Microwave power = 4 μW, field modulation width = 2 G.

Although we have tried to find the $\Delta M_s = \pm 1$ line for these radical pairs, we were not successful in detecting the signals for CH_3OH and CH_3OD. However, the spectrum of CD_3OD measured at 77 K after irradiation at 4.2 K clearly exhibits the perpendicular and parallel features of the radical pair spectrum as is shown in the overlay spectrum in Figure 3b. The average separation of the paired radicals is estimated to be 6.7 Å. The amount of paired radicals is crudely estimated to be 10% of the total radical yield. It was not possible to resolve the hyperfine structure so that the identification of the paired radicals was not possible.

Glassy Methanol Irradiated at 4.2 K. The glassy samples of methanol containing 5 mol % of water were irradiated at 4.2 K. Approximately the same amounts of hydroxymethyl radicals and trapped electrons are mainly formed. As a minor product, a slight indication of the signal from methyl radicals was observed in CH_3OD and in CH_3OH as is shown by the arrows in Figure 6a. However, the amount of $\dot{C}H_3$ may be less than 1%. The signal from $CH_3\dot{O}$ was not detectable. Upon exposing the sample to visible light, the signal from the hydroxymethyl radicals increased at the expense of the signal from the trapped electrons, the conversion being approximately quantitative. The relative abundance of the methyl to hydroxymethyl radicals slightly increased as is shown in Figure 6b. Although the conversion yield to $\dot{C}H_3$ is small, the net increase of $\dot{C}H_3$ with the decay of trapped electrons is of considerable importance from a view of radiation chemistry of methanol as will be discussed in a later section.

Discussion

Structure of $CH_3\dot{O}$. Usually a rotating methyl group gives four-line hyperfine structures with the intensity ratio of 1:3:3:1. However, at low temperature, the population of the torsional ground state becomes predominant, and the tunnel effect on the rotation of the methyl group makes the situation quite different as was predicted by Freed[9] and was observed by Miyagawa et al.[10,13] and others.[14]

Tunneling between the threefold minima of the methyl group rotation mixes the three states forming the A and E species for the torsional levels. The degeneracy of the E state is further removed by the hyperfine interaction. Because of the symmetry requirement for the total wave function, the nuclear spin eigenfunctions with A and E symmetries must be associated with the torsional A and E states. Therefore, the ESR hyperfine lines corresponding to the nuclear spin E state split into the two lines by the removal of the degeneracy of the torsional E levels, while the hyperfine lines corresponding to the nuclear spin A state are invariant. Thus, the conventional four-line spectrum becomes eight lines as is shown in Figure 7. Davidson and Miyagawa[10] have shown that the E-line splitting, δ, is expressed by the equation

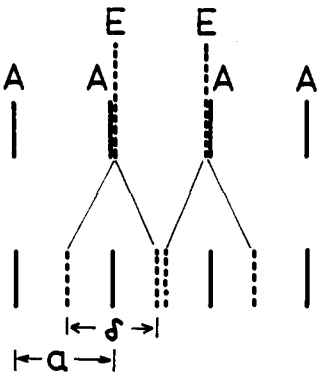

Figure 7. Eight-line hyperfine structures expected for the CH_3 group which undergoes quantum tunneling at low temperature. The tunneling frequency is assumed to be faster than the hyperfine frequency.

$$\delta = [(a - A_\gamma)^2 + (A_\alpha - A_\beta)^2/3]^{1/2} \quad (1)$$

where a is the A-line splitting and A_i's the methyl proton couplings in the equilibrium conformation. Now, if the methyl proton coupling in eq 1 obeys the following $\cos^2\theta$ rule with a constant term:

$$A_i = B_0 + B_2 \cos^2\theta_i \quad (2)$$

substitution of A_i in eq 1 by eq 2 gives a simple relation between the E-line splitting and B_2.

$$\delta = B_2/2 \quad (3)$$

On the other hand, A-line splitting, a, for the rapidly rotating methyl group becomes an average of A_i given by eq 2, that is

$$\begin{aligned} a = \langle A_i \rangle &= B_0 + B_2 \langle \cos^2\theta_i \rangle \\ &= B_0 + B_2/2 \end{aligned} \quad (4)$$

Equations 3 and 4 give

$$a - \delta = B_0 \quad (5)$$

Thus, the difference between the A- and E-line splittings gives the constant term B_0. If B_0 is zero as is assumed by Freed,[9] the A- and E-line splitting becomes equal and the seven-line spectrum with the intensity ratio of 1:1:1:2:1:1:1 results, provided that the tunneling splitting of the A and E levels associated with the torsional ground level is very much smaller than kT, resulting in equally populated A and E states. The hyperfine structure of $CH_3\dot{O}$ measured at 4.2 K is just what is expected from the theory. The observed spacing of the seven-line structure is not exactly equal. The A- and E-line splittings are determined to be 52 and 47 G, respectively. The difference between the two splittings is so small that the splitting of the central line was not resolved giving a seven-line structure with broader line width for the central line. The weaker intensity of the E lines indicates that the population of the E state is slightly smaller than that in the A state. Alternatively, the

Table I. Comparison of the g Tensor Elements for $CH_3\dot{O}$ with Those of $\dot{O}H$ Formed from Water of Crystallization in Sodium Hydrogen Maleate Trihydrate ($NaHM{\cdot}3H_2O$) and Dipotassium Fumarate Dihydrate ($K_2F{\cdot}2H_2O$)

	g_{max}	g_{int}	g_{min}	temp, K	ref
$\dot{O}H$ in $NaHM{\cdot}3H_2O$	2.062	2.008	2.003	77	15
	2.120	2.007	1.995	77	15
$\dot{O}H$ in $K_2F{\cdot}2H_2O$	2.092	2.009	2.003	15	16
av	2.093	2.008	2.000		
$CH_3\dot{O}$ in CH_3OH	2.088		1.999	4.2	present work

slight mixing of the classical rotation may account for the weaker E lines. From eq 3 and 5, B_0 and B_2 for the $\cos^2\theta$ rule of the methyl proton coupling in $CH_3\dot{O}$ are determined to be 5 and 94 G, respectively. These results may indicate that the CH_3 group in the $CH_3\dot{O}$ radical has C_3 symmetry.

The large positive g shift ($g_{max} = 2.088$) of $CH_3\dot{O}$ is characteristic of oxygen-centered π radicals in which the unpaired electron occupies the nonbonding p_π orbital of the oxygen atom having a large spin-orbit coupling constant. Promotion of an electron from the lone-pair orbital to the unpaired electron orbital gives a large positive g shift. It may be interesting to compare the g values with those of the $\dot{O}H$ radicals trapped in organic crystals. We have previously reported that $\dot{O}H$ radicals are formed from water of crystallization in the crystals of sodium hydrogen maleate trihydrate[15] and dipotassium fumarate dihydrate.[16] Table I shows the comparison of the g tensor elements with those of $\dot{O}H$ radicals. The g shift is strongly dependent on the crystalline field splitting of the two p_π orbitals of the oxygen atom. Since the g_{max} value (2.088) of $CH_3\dot{O}$ is nearly the same as the averaged g_{max} value of these $\dot{O}H$ radicals, the crystalline field splitting of the two p_π orbitals may be similar. The major contributor to the crystalline field splitting may be hydrogen bonding with the neighboring molecule. The large reduction of the hyperfine line width ($\Delta H_{1/2} \sim 6$ G) of $CH_3\dot{O}$ in CH_3OD as compared with that ($\sim$10 G) in CH_3OH may support this interpretation. From the similarity of the g tensor to that of $\dot{O}H$, one can conclude that $CH_3\dot{O}$ is the oxygen-centered π radical. The CH_3 group with C_3 symmetry is rapidly rotating around the C–O bond in which the lone pair and the unpaired electron orbitals of the oxygen atom are fixed in space.

It may be interesting to compare the methyl proton hyperfine coupling of the oxygen-centered π radicals $CH_3\dot{O}$ with those of the carbon- and nitrogen-centered π radicals (see Table II). A typical carbon-centered π radical, $CH_3\dot{C}H_2$, gives the methyl proton coupling of 27 G and the B_2 value in the $\cos^2\theta$ rule without a B_0 term is 58 G ($\rho_c = 0.92$ is assumed)as is reported by Fessenden and Schuler.[17] If it is assumed that $B_0 \approx 0$ and $\rho_0 = 1$ for $CH_3\dot{O}$, the B_2 value becomes 104 G. If ρ_0 is assumed to be 0.85, B_2 becomes as large as 122 G, in contrast to the carbon-centered π radicals. On the other hand, we have previously reported[18] that the nitrogen-centered π radical $RCH_2{}^+\dot{N}H_2$ in irradiated glycine exhibits a B_2 value as large as 99 G. Since the RCH_2 group in this radical has a fixed conformation, B_2 is determined from the two C–H_β proton couplings, assuming that the dihedral angle of the two C–H_β bonds is 120°. The spin density on the nitrogen atom is determined to be 0.7 from the nitrogen coupling tensor. As is tabulated in Table II, the B_2 value increases with decreasing the C–X bond distances. Since the origin of the β proton coupling is mainly due to the spin delocalization by hyperconjugation, the results indicate that the contribution from the no-bond structure having the C=X bond becomes larger with increasing double-bond character of the C—C, C—N, and C—O bonds.

Table II. Comparison of the β Proton Couplings in Carbon-, Nitrogen-, and Oxygen-Centered π Radicals

π radicals	a, G	ρ_x	B_2, G[a]	r_{C-X}, Å	ref
$CH_3\dot{C}H_2$	27	0.92	58	1.54	17
$CH_2R^+\dot{N}H_2$	23 (θ = 55°)	0.7	99	1.47	18
	11 (θ = 66°)				
$CH_3\dot{O}$	52	1.00	104	1.42	present work
		0.85	122		

[a] $a_{\beta H} = B_2 \cos^2\theta$ is assumed.

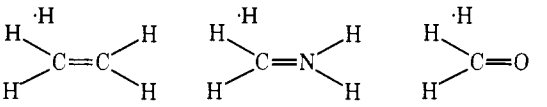

We have carried out the INDO MO calculation for $CH_3\dot{O}$ radicals. If one assumes the tetrahedral angle for ∠OCH, the geometry with $r_{CH} = 1.12$ Å and $r_{CO} = 1.36$ Å gives a minimum total energy but the coupling value obtained is 26.8 G, which is too small as compared with 52 G observed. However, the proton coupling is strongly dependent on the C–O bond distance. Although the complete energy minimization was not made by changing all the geometrical parameters, it was found that the geometry with ∠OCH = 114°, $r_{CH} = 1.16$ Å, and $r_{CO} = 1.26$ Å gives a coupling value of 48 G, which is fairly close to the observed value, although the total energy is 18 kcal/mol higher than that of the geometry mentioned above. If only the C–O bond distance is shortened without changing other geometry, a much larger increase of the total energy resulted ($\sim$50 kcal/mol). It seems that the C–O bond distance in $CH_3\dot{O}$ is considerably shorter while the C–H bond is longer than those in CH_3OH. In addition, it is likely that ∠OCH becomes larger than the tetrahedral value in $CH_3\dot{O}$.

Comparison with Alkoxy Radicals in DNA Constituents. In recent years, the ESR analysis of radiation damage centers produced in DNA constituents such as nucleosides and nucleotides has made great progress. Since Box and his coworkers have found substituted alkoxy radicals in irradiated serine[19] and in thymidine,[20] a number of alkoxy radicals have been found in irradiated nucleosides and nucleotides. The alkoxy radicals are formed at the oxygen atom of pentose, at which the phosphate group of the DNA main chain is attached as is shown below. This type of substituted alkoxy radicals

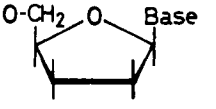

received considerable interest from a view of radiation biology, because this radical might be related to the DNA coil breakage.

Very recently, Bernhard et al.[21] have investigated the g and hyperfine coupling tensors of such alkoxy radicals determined for seven nucleotides and nucleosides as well as serine. As is shown in Table III, the averaged values of the g tensor elements for eight kinds of alkoxy radicals reported by them are in good agreement with the values of $CH_3\dot{O}$ determined by us. This means that the unpaired electron orbitals and the crystalline field splitting of the oxygen p_π orbitals in substituted alkoxy radicals trapped in nucleotides and nucleoside are similar to those of the fundamental radical $CH_3\dot{O}$ in methanol. Bernhard et al.[21] have also estimated the coefficient of the $\cos^2\theta$ rule of the CH_β proton coupling for these alkoxy radicals using the observed isotropic coupling, the dihedral angle expected from the crystallographic data, and other assumptions. From the eight kinds of alkoxy radicals, the crude values of B_0 and B_2 are estimated to be 0 and 90–116 G, respectively. According

Table III. Comparison of the g and Hyperfine Coupling Values of $CH_3\dot{O}$ and Substituted Alkoxy Radicals Trapped in Nucleotides and Nucleosides

	g_{max}	g_{int}	g_{min}	B_0, G	B_2, G	ref
alkoxy	2.076	2.006	1.998	~0[a]	90–116	21
radicals	± 0.014	± 0.001	± 0.002	5[b]	94	
$CH_3\dot{O}$	2.088		1.999	5[c]	94	present work

[a] Obtained from the eight kinds of substituted alkoxy radicals. [b] Obtained from alkoxy radicals in adenosine hydrochloride. [c] Obtained from the A- and E-line splittings.

to Bernhard et al.,[21] the data obtained from the alkoxy radical in adenosine hydrochloride are most informative and give B_0 = 5 G and B_2 = 94 G. This is exactly the same as those determined from the A- and E-line splittings of $CH_3\dot{O}$ in the present work. From these similarities, it is concluded that the abnormally large hyperfine coupling in alkoxy radicals in nucleotides and nucleosides is characteristic of the oxygen-centered π radicals.

Structure of Radical Pairs. As is described in the foregoing section, the hyperfine structure of $\Delta M_s = \pm 2$ spectrum of radical pairs changes from six to five lines owing to the radical conversion from $\dot{C}H_3$ to $\dot{C}H_2OH$. It is to be noted that this change of the spectrum is accompanied by the shift of the resonance position; that is, the center of the hyperfine lines moves about 3 G to the high-field side after the conversion. This indicates that the interradical distance becomes a bit larger after the conversion.

The resonance position of the $\Delta M_s = \pm 2$ spectrum is not exactly one-half of the resonance field of the $\Delta M_s = \pm 1$ spectrum when the electron-electron dipolar interaction is considerably large, because of the mixing of the $M_s = 0$ and $M_s = \pm 1$ states. The resonance position shifts to the lower field side with increasing dipolar interaction and the shift from the exact half field is given by[1,22]

$$\delta H_{1/2} = (d_\perp{}^2/6H_{1/2})[1 - (1 - 3\cos^2\theta)^2/4] \quad (6)$$

$$d_\perp = 3g\beta/2r^3 \quad (7)$$

where $d_\perp$ is the perpendicular component of the dipole–dipole splitting, θ is the angle between the external field and $\vec{r}$, r is the interradical distance, and $H_{1/2}$ is the half-field resonance position. For a polycrystalline sample, the averaged shift for all the orientations has to be obtained taking the weight coming from the angular dependence of the intensity of the $\Delta M_s = \pm 2$ transition into consideration. The intensity ratio of the $\Delta M_s = \pm 2$ and ± 1 transition is given by[1,12,22]

$$I_2/I_1 = (d_\perp \sin 2\theta/2H_{1/2})^2 \quad (8)$$

where I_1 is for the sum of the two $\Delta M_s = \pm 1$ transitions, $|-1\rangle \leftrightarrow |0\rangle$ and $|0\rangle \leftrightarrow |+1\rangle$, and I_2 for the $\Delta M_s = \pm 2$ transition. The weighted average of $\delta H_{1/2}$ is obtained to be

$$\langle \delta H_{1/2} \rangle = -d_\perp{}^2/7H_{1/2} \quad (9)$$

for nonoriented samples. The averaged value of I_2/I_1 for all the orientations is given by[12]

$$\langle I_2/I_1 \rangle = (2/15)(d_\perp/H_{1/2})^2 \quad (10)$$

As stated before, the stable radical pair at 77 K found in CD_3OD has a separation of 6.7 Å. The second-order shift, $\langle \delta H_{1/2} \rangle$, expected for this pair is estimated to be 0.8 G from eq 9. The stable radical pairs in CH_3OH and CH_3OD show nearly the same shift. Therefore, assuming that the separation of the stable radical pairs in CH_3OH and CH_3OD is 6.7 Å as in CD_3OD, the second-order shifts of the unstable radical pair were estimated to be 3.9 G for CH_3OD and 4.4 G for CH_3OH, from the difference in the resonance field of the stable and unstable radical pairs. These values for $\langle \delta H_{1/2} \rangle$ give 5.1 and 5.0 Å for the separation of the unstable radical pair. Since the principal directions of the dipole–dipole interaction tensor are not determined in this study using polycrystalline samples, the definite correspondence to the crystal structure is not possible. However, as a probable correspondence, the following radical pair and its conversion are suggested from the experimental data described above.

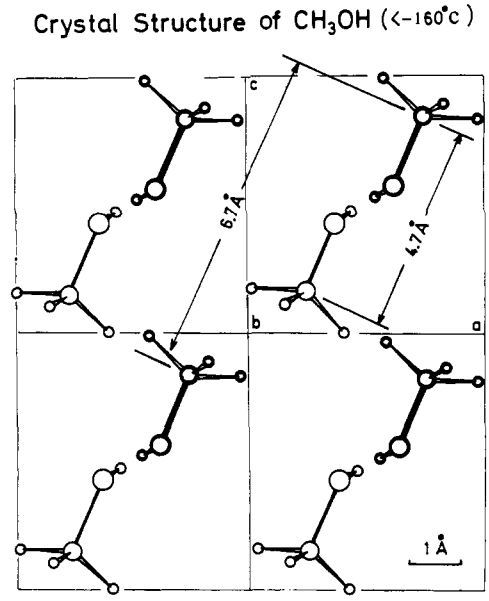

Figure 8. Crystal structure of CH_3OH in the low-temperature (158 K) phase cited from ref 23. The positions of hydrogen atoms are assumed to be staggered with respect to the OH and CH_3 groups. A linear hydrogen bond is assumed.

Shown in Figure 8 is the crystal structure of methanol in the low-temperature phase determined by Tauer and Lipscomb[23] at −160 °C. The crystal is monoclinic with the space group $P2_1/m$ and the unit cell with a = 4.53, b = 4.69, and c = 4.91 Å and β = 90° contains two molecules, which are linked by a hydrogen bond as is shown in Figure 8. Since the positions of hydrogen atoms are not determined, we have assumed a staggered conformation and a linear hydrogen bond to locate the hydrogen atoms. The intercarbon distance of the hydrogen-bonded pair in the unit cell is 4.75 Å. It is likely that the $\dot{C}H_3\cdots\dot{C}H_2OH$ pair is formed between this hydrogen-bonded pair. It is suggested that the methyl carbon atom slightly shifts along the broken C–O bond giving the intercarbon distance of about 5 Å and that the p orbital directs along the broken C–O bond. In our previous study, it has been shown that the unpaired electron orbital of the $\dot{C}H_3$ radicals in $CH_3CO_2Li\,2H_2O$ directs along the broken C–C bond.[24] Now, if the methyl radical abstracts an hydrogen atom from the closest neighboring methyl group sitting in front of the unpaired electron orbital, the $\dot{C}H_2OH\cdots\dot{C}H_2OH$ pair with a separation of 6.75 Å is expected to be formed from the crystal structure, as is indicated in Figure 9. The observed separation of the stable radical pair just coincides with this separation. The crystal structure shows that this seems to be the only possibility that a radical pair with a separation of 5 Å is first formed and then

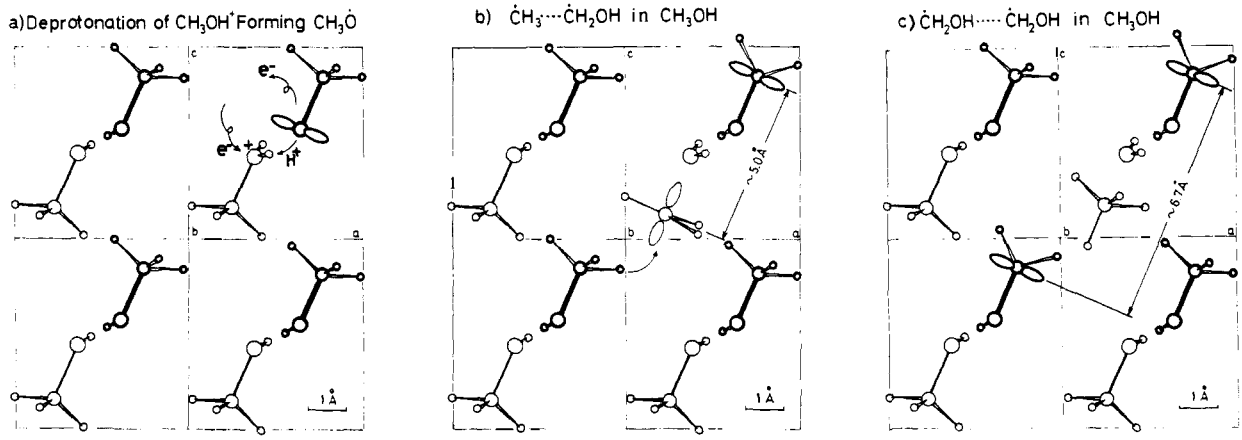

Figure 9. Proposed mechanism and structure of radical pairs formed in crystalline CH_3OH X-irradiated at 4.2 K: (a) electron ejection and proton transfer process; (b) unstable radical pair, $\dot{C}H_2OH\cdots\dot{C}H_3$; (c) stable radical pair, $\dot{C}H_2OH\cdots\dot{C}H_2OH$.

it converts into a pair with a separation of 6.75 Å by a reasonable hydrogen atom abstraction reaction by $\dot{C}H_3$.

Mechanism of Radiolysis. Formation of methoxy radicals has been postulated in the radiolysis of methanol for a long time and direct evidence has been obtained in this work, although indirect evidence has been suggested from spin-trapping experiments.[25] On the other hand, formation of methyl radicals as a major product was unexpected. The mechanism of methanol radiolysis proposed so far does not seem to involve the formation of methyl radicals. After completing the work, we have become aware of the papers recently reported by Symons and his co-workers[26] in which the formation of $\dot{C}D_3$ and $\dot{C}H_3$ in irradiated CD_3OD containing a small amount of CH_3OH has been described.

Since an appreciable amount of methyl radicals was not formed in the glassy sample which gives trapped electrons and the net increase of methyl radicals was observed with the photobleaching of the trapped electrons, formation of methyl radical may be related to the reaction of electrons. It has been customarily postulated that the detrapped electron is captured by methanol followed by the dissociative process (11):[27]

$$e^- + CH_3OH \rightarrow CH_3O^- + H \quad (11)$$

$$\dot{H} + CH_3OH \rightarrow \dot{C}H_2OH + H_2 \quad (12)$$

and hydrogen atoms react with CH_3OH forming $\dot{C}H_2OH$. Our result suggests that the following dissociative process may be of importance:

$$e^- + CH_3OH \rightarrow \dot{C}H_3 + OH^- \quad (13)$$

However, reaction 13 does not seem to account for the difference between the crystalline and glassy states. It is suggested that proton transfer to methanol anion takes place across the hydrogen bond followed by the dissociative process (15) in the crystalline state.

$$e^- + CH_3OH \rightarrow [CH_3OH]^- \quad (14)$$

$$[CH_3OH]^- + CH_3OH \rightarrow \dot{C}H_3 + H_2O + CH_3O^- \quad (15)$$

This process must give an isolated $\dot{C}H_3$ radical away from the primary cation, if an electron travels a fairly long distance before being captured. An isolated $CH_3\dot{O}$ radical is considered to be formed from this primary cation by a proton-transfer reaction (16) through the intermolecular hydrogen bond.

$$CH_3OH^+ + CH_3OH \rightarrow CH_3\dot{O} + CH_3OH_2^+ \quad (16)$$

We have often observed such proton-transfer reactions triggered by electron capture and electron loss in a number of hydrogen-bonded crystals.[16,18,28] These proton transfer reactions (15 and 16) must more easily take place in the crystalline phases.

$CH_3\dot{O}$ is stabilized in the crystalline state at low temperature at which only the lowest torsional level ($v = 0$) is populated. However, it is suggested that $CH_3\dot{O}$ converts into $\dot{C}H_2OH$ by intramolecular hydrogen atom transfer when the population of the excited torsional level increases with increasing temperature. In other words, with increasing amplitude of the torsional oscillation, the overlapping of the unpaired electron orbital with the C-H bond increases resulting in the intramolecular hydrogen atom hopping. It is hard to believe that $CH_3\dot{O}$ abstracts a hydrogen atom from the neighboring CH_3 group, because there is no methyl group adjacent to the oxygen atom as is seen in the crystal structure shown in Figure 8. The diffusion of $CH_3\dot{O}$ at such low temperature may not be possible Another important factor for stabilizing $CH_3\dot{O}$ may be a hydrogen bonding which fixes the unpaired electron orbital in space. In the glassy state, the hydrogen-bonded chain of the methanol molecules may become greatly disordered resulting in a weaker hydrogen bond and $CH_3\dot{O}$ may not be stabilized in the glassy sample where the unpaired electron orbital may not be tightly fixed in space. These may be the reasons why $CH_3\dot{O}$ is not observed in the glassy state. Although reaction 16 involving proton transfer across the hydrogen bond may proceed more easily in the regular crystalline state, some other pathway from the primary cation to $\dot{C}H_2OH$ might also be involved in the glassy state.

In the crystalline state in which the ejected electron is not physically trapped, a considerable amount of electrons must recombine with cations. If reaction 16 takes place before the recombination, the electrons may be neutralized with $CH_3OH_2^+$ forming $\dot{C}H_3$ and H_2O.

$$e^- + CH_3OH_2^+ \rightarrow \dot{C}H_3 + H_2O \quad (17)$$

$$CH_3\dot{O} \rightarrow \dot{C}H_2OH \quad (18)$$

There must be $CH_3\dot{O}$, which may be linked by the hydrogen bond with $CH_3OH_2^+$ if the successive proton transfer does not take place along the hydrogen-bonded chain before neutralization. Then the radical pair between $\dot{C}H_3$ and $CH_3\dot{O}$ may be formed. However, an excess energy liberated from this neutralization reaction may be used to excite the torsional level of the neighboring $CH_3\dot{O}$ to isomerize into $\dot{C}H_2OH$ (18). Thus, the $\dot{C}H_3\cdots\dot{C}H_2OH$ radical pair is formed between the two neighboring molecules linked by a hydrogen bond. When the successive proton transfer takes place along the hydrogen-bonded chain before neutralization, isolated $\dot{C}H_3$ radical may be formed from reaction 17 as well.

If the proton transfer reaction 16 does not take place before

neutralization, excited methanol may be formed by reaction 19 and some may decompose into methyl and ȮH radicals, as in $\dot{C}H_3$ formation by UV irradiation of crystalline methanol.[29]

$$CH_3OH^+ + e^- \rightarrow CH_3OH^* \quad (19)$$

$$CH_3OH^* \rightarrow \dot{C}H_3 + \dot{O}H \quad (20)$$

$$\dot{O}H + CH_3OH \rightarrow \dot{C}H_2OH + H_2O \quad (21)$$

If ȮH radical selectively abstracts a hydrogen atom from the neighboring methyl group because of a smaller bond dissociation energy than that of the OH bond, the radical pair between $\dot{C}H_3$ and $\dot{C}H_2OH$ may also be formed. The hot abstraction of a hydrogen atom from the OH bond which is hydrogen bonded to the broken OH group may also take place. In this case, one has to assume that the isomerization reaction (18) of $CH_3\dot{O}$ into $\dot{C}H_2OH$ takes place following the reaction

$$\dot{O}H + CH_3OH \rightarrow CH_3\dot{O} + H_2O \quad (22)$$

The signal from trapped hydrogen atoms was detected neither in the crystalline nor in the glassy methanol irradiated and measured at 4.2 K. This does not always mean that hydrogen atoms are not formed. Recently, we have shown that thermal hydrogen atoms can abstract a hydrogen atom from C_2H_6 even at 10–20 K.[5] It is suggested that hydrogen atoms react with CH_3OH even after thermalization at 4.2 K. Hydrogen atoms may be formed from reaction 11 as well as the charge neutralization reaction

$$e^- + CH_3OH_2^+ \rightarrow CH_3OH + \dot{H} \quad (23)$$

Although the fate of hydrogen atoms is not clear, besides reaction 12, the following reactions may also be possible:

$$\dot{H} + CH_3OH \rightarrow \dot{C}H_3 + H_2O \quad (24)$$

$$\dot{H} + CH_3OH \rightarrow CH_3\dot{O} + H_2 \quad (25)$$

Tunneling Abstraction Reaction by $\dot{C}H_3$. The hydrogen abstraction reaction by thermal methyl radicals from the neighboring CH_3OH forming $\dot{C}H_2OH$ has been observed below 77 K for both the isolated and paired methyl radicals. The half-lives crudely estimated are 9 min at 77 K and 1 h at 4.2 K. On the other hand, $\dot{C}D_3$ in CD_3OD is quite stable at 77 K, and the half-life may be longer than a few days. According to the recent paper by Symons and his co-workers,[27] $\dot{C}H_3$ is stabilized at 77 K in the matrices of CD_3OD. The large mass effect in the hydrogen abstraction reaction at low temperatures and the fact that reaction of $\dot{C}H_3$ proceeds even at 4.2 K may suggest that the reaction proceeds by the tunnel effect. These results quite resemble the behavior of $\dot{C}H_3$ radicals formed from CH_3I in CH_3OH glasses reported by Williams and his co-workers.[30] Recently, they have measured the temperature dependence of the rate constant from 100 to 15 K.[31] The rate constants become nearly temperature independent below 40 K. A similar observation was also made by us[4] for hydrogen atom transfer reactions involved in the iminoxy radical pair conversion in irradiated dimethylglyoxime in the temperature range from 140 to 4.2 K. The strongly bent Arrhenius plot is interpreted by the tunnel effect in the hydrogen atom transfer reaction.[4,30] The half-lives of $\dot{C}H_3$ in glassy methanol are estimated by Williams' group to be 4 and 30–50 min at 77 and below 40 K, respectively. The half-lives seems to be considerably shorter in the glassy methanol, reflecting the difference in the rigidity of the matrices. Studies of the hydrogen atom transfer reactions in crystalline phases, where the relative geometry of the reactants is known, may be of a great importance for elucidation of the nature of the tunnel effect in chemical reactions.

Acknowledgment. We wish to thank Mr. K. Nunome and Mr. H. Muto for their assistance in the low-temperature experiments.

References and Notes

(1) Iwasaki, M.; Toriyama, K.; Muto, H.; Nunome, K. *J. Chem. Phys.* **1976**, *65*, 596–606. *Chem. Phys. Lett.* **1976**, *39*, 90–94.
(2) Nunome, K.; Muto, H.; Toriyama, K.; Iwasaki, M. *Chem. Phys. Lett.* **1976**, *39*, 542–546.
(3) Iwasaki, M.; Toriyama, K.; Numone, K.; Fukaya, M.; Muto, H. *J. Phys. Chem.* **1977**, *81*, 1410–1417.
(4) Toriyama, K.; Nunome, K.; Iwasaki, M. *J. Am. Chem. Soc.* **1977**, *99*, 5823–5824.
(5) Iwasaki, M.; Toriyama, K.; Muto, H.; Nunome, K. *Chem. Phys. Lett.* **1978**, *56*, 494–496.
(6) Kevan, L. *Adv. Radiat. Chem.* **1974**, *4*, 181–345.
(7) Pshezhetskii, S. Ya.; Kotov, A. G.; Millinchuk, V. K.; Robinskii, V. A.; Tupikov, V. I. "EPR of Free Radicals in Radiation Chemistry", Wiley: New York, 1974; pp 189–202.
(8) Iwasaki, M.; Toriyama, K. *J. Am. Chem. Soc.* **1978**, *100*, 1964–1965.
(9) Freed, J. H. *J. Chem. Phys.* **1965**, *43*, 1710–1720.
(10) Davidson, R. B.; Miyagawa, I. *J. Chem. Phys.* **1970**, *52*, 1727–1732.
(11) Kurita, K. *J. Chem. Phys.* **1964**, *41*, 3926–3927. *Nippon Kagaku Zasshi* **1964**, *85*, 833–842.
(12) Iwasaki, M.; Ichikawa, T.; Ohmori, T. *J. Chem. Phys.* **1969**, *50*, 1984–1990.
(13) Gamble, W. L.; Miyagawa, I.; Hartman, R. L. *Phys. Rev. Lett.* **1968**, *20*, 415–418.
(14) (a) Wells, J. W.; Box, H. C. *J. Chem. Phys.* **1968**, *48*, 2542–2546. (b) Clogh, S.; Poldy, F. *ibid.* **1969**, *51*, 2076–2084. (c) Iwasaki, M.; Nunome, K.; Muto, H.; Toriyama, K., *ibid.* **1971**, *54*, 1839–1840.
(15) Toriyama, K.; Iwasaki, M. *J. Chem. Phys.* **1971**, *55*, 1890–1894.
(16) Iwasaki, M.; Minakata, K.; Nunome, K.; Tagami, K. *J. Chem. Phys.* **1972**, *57*, 3187–3193.
(17) Fessenden, R. W.; Schuler, R. H. *J. Chem. Phys.* **1963**, *39*, 2147–2195.
(18) Nunome, K.; Muto, H.; Toriyama, K.; Iwasaki, M. *J. Chem. Phys.* **1976**, *65*, 3805–3807.
(19) Lee, J. Y.; Box, H. C. *J. Chem. Phys.* **1973**, *59*, 2509–2512.
(20) Box, H. C.; Budzinskii, E. E. *J. Chem. Phys.* **1975**, *69*, 197–199.
(21) Bernhard, W. A.; Close, D. M.; Huttermann, J.; Zehner, H. *J. Chem. Phys.* **1977**, *67*, 1211–1219.
(22) Iwasaki, M. *J. Magn. Reson.* **1974**, *16*, 417–423.
(23) Tauer, K. J.; Lipscomb, W. N. *Acta Crystallogr.* **1952**, *5*, 606–612.
(24) Toriyama, K.; Nunome, K.; Iwasaki, M. *J. Chem. Phys.* **1976**, *64*, 2020–2026.
(25) (a) Wargon, J. A.; Williams, F. *J. Am. Chem. Soc.* **1972**, *94*, 7917–7918. (b) Schlick, S.; Kevan, L. *Chem. Phys. Lett.* **1976**, *38*, 505–509. (c) Shiotani, M.; Murabayashi, S.; Sohma, J. *Int. J. Radiat. Phys. Chem.* **1976**, *8*, 485–495. (c) Sargent, F. P.; Gardy, E. M. *J. Phys. Chem.* **1976**, *80*, 854–856.
(26) Symons, M. C. R.; Eastland, G. W. *J. Chem. Res. (S)* **1977**, 254–255.
(27) Shida, T.; Hamil, W. H. *J. Am. Chem. Soc.* **1966**, *88*, 3689–3694.
(28) (a) Iwasaki, M. *MTP Int. Rev. Sci.: Phys. Chem., Ser. One* **1972**, *4*, 317–364. (b) Iwasaki, M.; Minakata, K.; Toriyama, K. *J. Am. Chem. Soc.* **1971**, *93*, 3533–3534. (c) Minakata, K.; Iwasaki, M. *J. Chem. Phys.* **1972**, *57*, 4758–4763. (d) Muto, H.; Iwasaki, M. *ibid.* **1973**, *59*, 4821–4829. (e) Muto, H.; Nunome, K.; Iwasaki, M. *ibid.* **1974**, *61*, 1075–1077. (f) Muto, H.; Nunome, K.; Iwasaki, M. *ibid.* **1974**, *61*, 5311–5314. (g) Iwasaki, M.; Muto, H. *ibid.* **1974**, *61*, 5315–5320. (h) Iwasaki, M.; Toriyama, K. *Chem. Phys. Lett.* **1976**, *41*, 59–63. (i) Muto, H.; Iwasaki, M.; Takahashi, Y. *J. Chem. Phys.* **1977**, *66*, 1943–1952.
(29) Sullivan, S. P. J.; Koski, W. S. *J. Am. Chem. Soc.* **1962**, *84*, 1–4.
(30) Campion, A.; Williams, F. *J. Am. Chem. Soc.* **1972**, *94*, 7633–7637.
(31) Hudson, R. L.; Shiotani, M.; Williams, F. *Chem. Phys. Lett.* **1977**, *48*, 193–196.